The RNA-binding protein Fus directs translation of localized mRNAs in APC-RNP granules

Kyota Yasuda,[1] Huaye Zhang,[2] David Loiselle,[3] Timothy Haystead,[3] Ian G. Macara,[4] and Stavroula Mili[1]

[1]Laboratory of Cellular and Molecular Biology, National Cancer Institute, National Institutes of Health, Bethesda, MD 20892
[2]Department of Neuroscience and Cell Biology, Robert Wood Johnson Medical School, Rutgers, The State University of New Jersey, Piscataway, NJ 08854
[3]Department of Pharmacology and Cancer Biology, Duke University, Durham, NC 27710
[4]Department of Cell and Developmental Biology, Vanderbilt University Medical Center, Nashville, TN 37232

RNA localization pathways direct numerous mRNAs to distinct subcellular regions and affect many physiological processes. In one such pathway the tumor-suppressor protein adenomatous polyposis coli (APC) targets RNAs to cell protrusions, forming APC-containing ribonucleoprotein complexes (APC-RNPs). Here, we show that APC-RNPs associate with the RNA-binding protein Fus/TLS (fused in sarcoma/translocated in liposarcoma). Fus is not required for APC-RNP localization but is required for efficient translation of associated transcripts. Labeling of newly synthesized proteins revealed that Fus promotes translation preferentially within protrusions. Mutations in Fus cause amyotrophic lateral sclerosis (ALS) and the mutant protein forms inclusions that appear to correspond to stress granules. We show that overexpression or mutation of Fus results in formation of granules, which preferentially recruit APC-RNPs. Remarkably, these granules are not translationally silent. Instead, APC-RNP transcripts are translated within cytoplasmic Fus granules. These results unexpectedly show that translation can occur within stress-like granules. Importantly, they identify a new local function for cytoplasmic Fus with implications for ALS pathology.

Introduction

Numerous mRNAs are regulated through subcellular targeting and local control of their translation (Holt and Bullock, 2009). RNA localization impacts many processes including cell polarity (Li et al., 2008; Nagaoka et al., 2012), migration (Shestakova et al., 2001), neuronal axon growth and pathfinding (Leung et al., 2006; Hengst et al., 2009), and mitotic spindle assembly (Blower et al., 2007). Defects in localization have been implicated in diseases such as mental retardation and cancer metastasis (Bassell and Warren, 2008; Vainer et al., 2008).

We previously described a pathway that targets many RNAs to cellular protrusions (Mili et al., 2008). A central component of this pathway is the tumor suppressor protein adenomatous polyposis coli (APC; Näthke, 2004). At protrusive areas, and specifically at the plus-ends of detyrosinated microtubules, APC associates with multiple RNAs (such as Pkp4, Rab13, Kank2, and Ddr2) and proteins (such as FMRP and PABP1) to form APC-containing ribonucleoprotein complexes (APC-RNPs; Mili et al., 2008). This APC function might mediate effects on cell migration (Sansom et al., 2004; Kroboth et al., 2007; Harris and Nelson, 2010), and is distinct from its canonical function in the Wnt pathway where it regulates β-catenin degradation (Kennell and Cadigan, 2009).

APC-RNPs are concentrated in granules that likely contain many different transcripts (Mili et al., 2008). Several RNA granule types exist that share common components and are either constitutively present (such as neuronal transport granules and P-bodies) or form in response to stress (stress granules). They are sites where RNAs are silenced through translational repression or decay (Anderson and Kedersha, 2008; Buchan and Parker, 2009). Other types of higher order RNA–protein assemblies are also formed by aggregation-prone RNA-binding proteins such as Fus (fused in sarcoma) and TDP43 in neurodegenerative diseases (Lagier-Tourenne et al., 2010; Liu-Yesucevitz et al., 2011).

Correspondence to Stavroula Mili: voula.mili@nih.gov

Abbreviations used in this paper: AHA, azidohomoalanine; ALS, amyotrophic lateral sclerosis; APC, adenomatous polyposis coli; APC-RNP, APC-containing ribonucleoprotein complex; FISH, fluorescence in situ hybridization; FTLD, frontotemporal lobar degeneration; Fus, fused in sarcoma; HPG, homopropargylglycine; KD, knockdown; TLS, translated in liposarcoma.

The Rockefeller University Press $30.00
J. Cell Biol. Vol. 203 No. 5 737–746
www.jcb.org/cgi/doi/10.1083/jcb.201306058

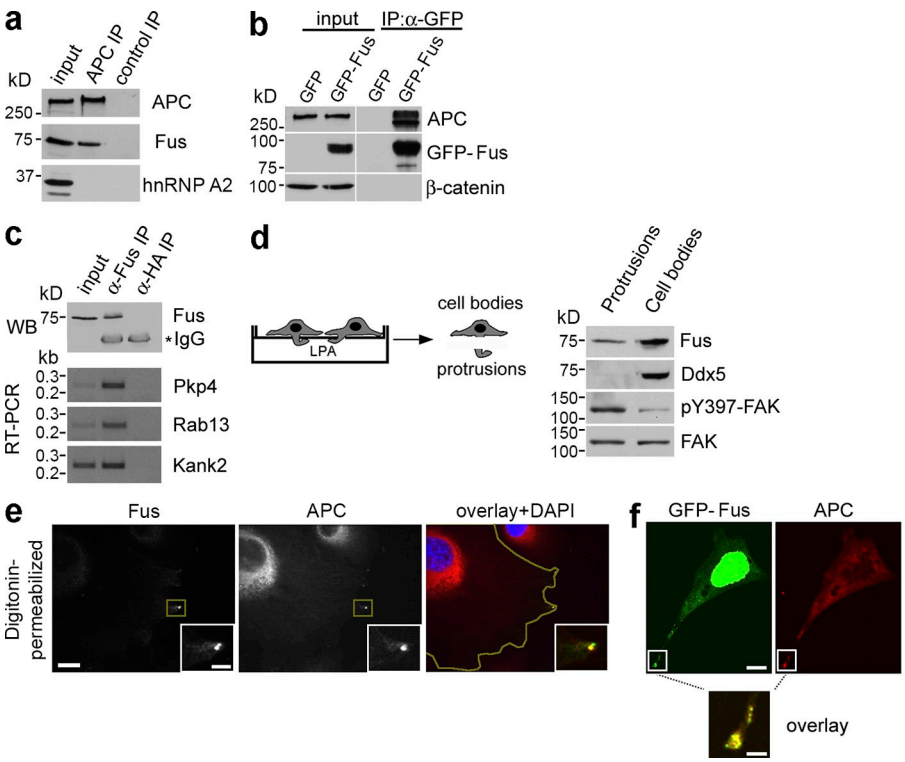

Figure 1. **The RNA-binding protein Fus is a component of APC-RNPs at cell protrusions.** NIH/3T3 cells untransfected (a and c) or transfected with GFP or GFP-Fus (b) were immunoprecipitated (IP) with the indicated antibodies and analyzed by Western blot (a–c, top panel) or by RT-PCR (c, bottom panels). (d) NIH/3T3 cells were plated on microporous filters, induced to migrate by addition of LPA, and protrusions and cell bodies were isolated and analyzed by Western blot. (e) NIH/3T3 cells were immunostained to detect endogenous Fus and APC. Insets: magnification of the boxed protrusive area. Yellow line in overlay panel: cell outline (f) GFP-Fus–expressing cells immunostained to detect APC. Bars, 10 µm (insets, 3 µm).

Dominant mutations in Fus are found in amyotrophic lateral sclerosis (ALS) cases, and Fus is also the pathological protein in types of frontotemporal lobar degeneration (FTLD; Lagier-Tourenne et al., 2010; Mackenzie et al., 2010). The disease hallmark is Fus-containing inclusions, which share components with stress granules, suggesting that alterations in RNA metabolism might underlie disease pathogenesis (Andersson et al., 2008; Bosco et al., 2010; Dormann et al., 2010).

We show here that Fus is a component of APC-RNPs at cell protrusions and is required for their efficient translation. Using a metabolic labeling approach to mark newly synthesized proteins, we show that Fus preferentially affects translation within protrusions. Cytoplasmic granules formed by either overexpression of wild-type Fus or by expression of ALS mutants of Fus preferentially recruit APC-RNPs. Strikingly, these granules are not translationally silent. Instead, we show that translation occurs within cytoplasmic Fus granules leading to local protein production from APC-RNPs.

Results and discussion

Fus is a component of APC-RNPs at cell protrusions

To find additional APC-RNP components, we identified by mass spectrometry proteins that coimmunoprecipitate with APC from mouse fibroblasts. One candidate was the RNA-binding protein Fus (Fig. S1 a). Indeed, endogenous Fus, but not hnRNPA2, associates with immunoprecipitated APC (Fig. 1 a). Additionally, immunoprecipitated GFP-Fus associates specifically with APC, but not with β-catenin (Fig. 1 b), indicating that Fus is not part of the destruction complex in the Wnt pathway. Furthermore, Fus associates with RNAs that are present in APC-RNPs (Pkp4, Rab13, Kank2; Fig. 1 c; Mili et al., 2008). Consistent with the limited sequence specificity and large number of RNA targets described for Fus (Lagier-Tourenne et al., 2012; Rogelj et al., 2012), we find little specificity for Fus with regards to RNA binding. Interestingly, however, quantitation of the efficiency of binding revealed that Fus associates preferentially with RNAs enriched in protrusions (Pkp4, Rab13, Kank2) compared with RNAs not enriched in protrusions (Actb, Arpc3; Fig. S1 b; Mili et al., 2008).

To test whether Fus is present in protrusions, we isolated protrusions and cell bodies from cells induced to migrate on microporous filters (Fig. 1 d). Indeed, Fus was present within protrusions, whereas Ddx5, a nuclear shuttling RNA-binding protein analogous to Fus, was not (Fig. 1 d). Phosphorylated Y397-FAK marks the isolated protrusions (Mili et al., 2008). We additionally immunostained actively spreading cells using different Fus antibodies (Fig. 1 e and Fig. S1 c). To enhance our ability to detect cytoplasmic Fus, the cells were permeabilized with digitonin to prevent antibody access into the nucleus, where most of Fus resides at steady state (Fig. 1 f; Dormann et al., 2010). Fus was detected in the cytoplasm concentrated in peripheral granules that colocalized with APC (Fig. 1 e and Fig. S1, c and d). Similar results were obtained with exogenous GFP-Fus (Fig. 1 f). Taken together, these data strongly indicate that cytoplasmic Fus is mostly present at cell protrusions associated with APC-RNPs.

Fus preferentially regulates translation at cell protrusions

To determine the function of Fus in APC-RNPs, we silenced Fus expression (Fig. 2 a) and tested for effects on APC-RNP

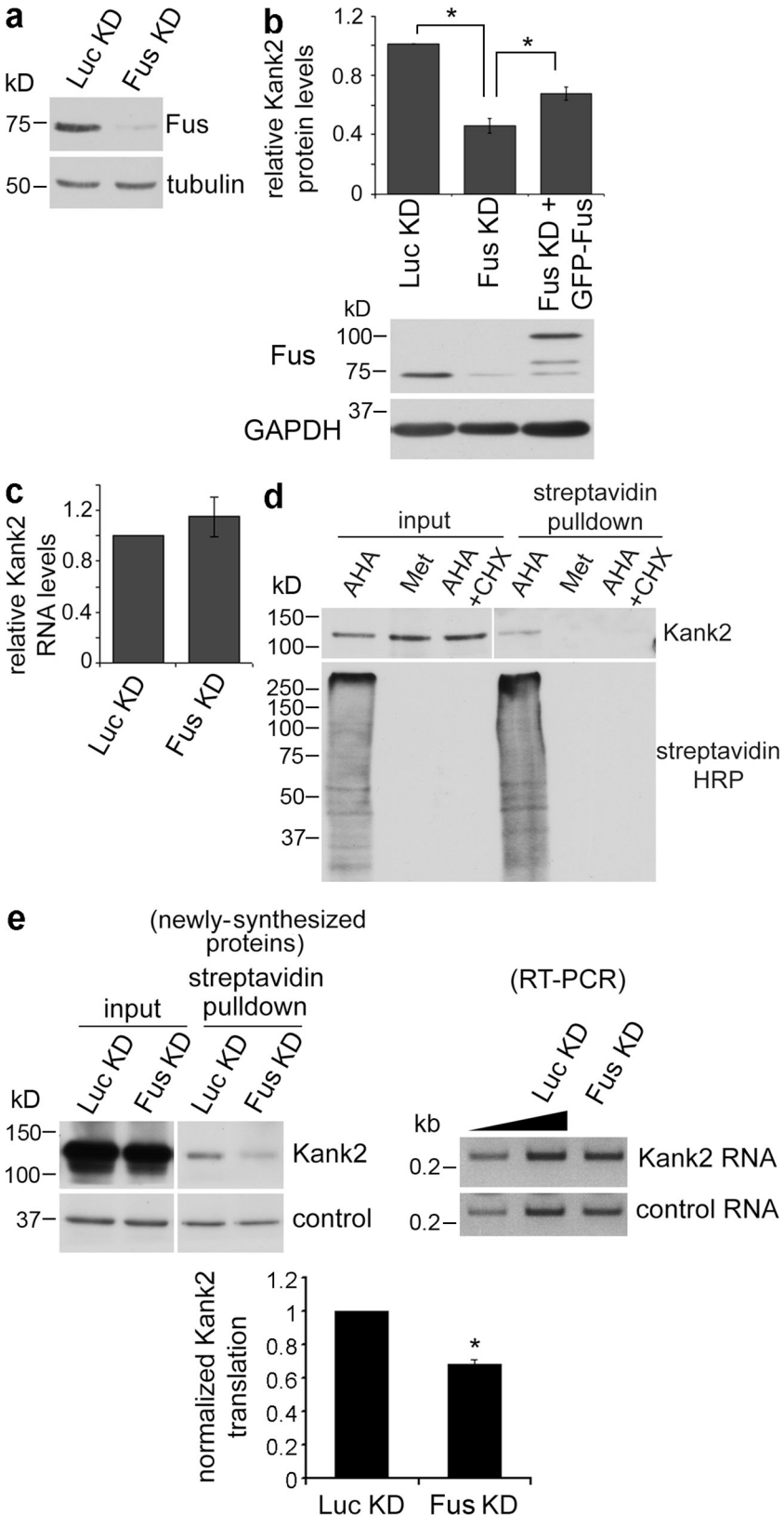

Figure 2. **Fus is required for efficient translation of the Kank2-localized mRNA.** (a) Western blot of NIH/3T3 cells stably expressing short hairpin RNAs against luciferase (Luc KD) or Fus (Fus KD). (b and c) Kank2 protein (b, top) and RNA levels (c) were detected in Luc KD, Fus KD, or Fus KD cells reexpressing GFP-Fus. $n = 5$. *, $P < 0.05$ by Student's t test. (b, bottom) Western blot showing levels of reexpressed GFP-Fus (d) Cells were labeled with AHA, methionine (Met), or AHA in the presence of cycloheximide for 30 min. AHA-labeled proteins in lysates were biotinylated and purified with streptavidin beads. Kank2 or total biotinylated proteins (streptavidin-HRP) were detected. (e) Newly synthesized proteins from Luc KD or Fus KD cells were isolated as in d (left), and the indicated RNAs were detected by RT-PCR (middle). Graph shows Kank2 protein/RNA after normalization to the corresponding controls (GAPDH/tubulin). *, $P = 0.006$ by Student's t test.

localization. We used either RT-PCR of isolated protrusions or fluorescence in situ hybridization (FISH). All RNAs examined (Rab13, Pkp4, Kank2, Ddr2, and TAT-SF1) remained enriched in protrusions of Fus knockdown (Fus KD) cells similarly to the control Luc KD cells (expressing short hairpin RNAs against luciferase; Fig. S1 e). Furthermore, by FISH, the peripheral concentration of the Rab13 and Ddr2 RNAs remained unchanged upon Fus depletion (Fig. S1 f). Therefore, Fus is not required for localization of RNAs at cell protrusions.

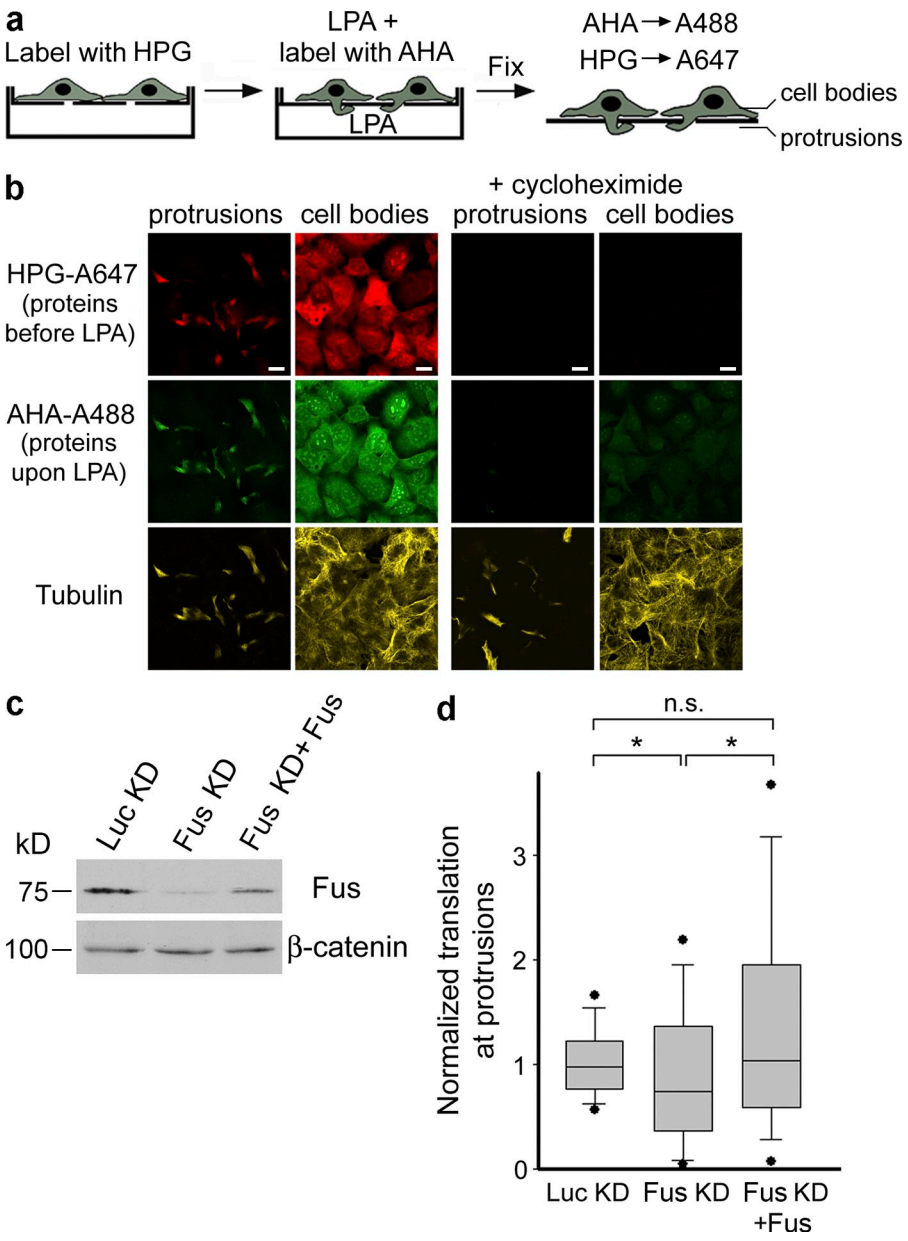

Figure 3. **Fus is required for efficient translation in cell protrusions.** (a) Diagram showing labeling scheme of cells on microporous filters. (b) Confocal images of protrusions or cell bodies of cells labeled as in panel a with or without cycloheximide. Cells were also immunostained to detect Tubulin. (c) Western blot of Fus levels in control, Fus KD cells, and Fus KD cells reexpressing Fus. (d) Box-plot graph showing values of normalized translation at protrusions of the indicated cell types. *, $P < 0.05$ by Mann-Whitney test; n.s.: not significant. Bars, 16 µm.

We next examined whether Fus affects APC-RNP translation. We focused on the protein produced from the Kank2-localized RNA, for which high affinity antibodies are available. Strikingly, Fus depletion significantly reduced whole-cell Kank2 protein levels without affecting the corresponding mRNA levels (Fig. 2, b and c). Re-expression of shRNA-resistant GFP-Fus into Fus KD cells partially rescued this effect, to a level corresponding to the cell transfection efficiency (40–50%), suggesting that Fus is required for efficient translation of Kank2 mRNA (Fig. 2 b).

To test directly a role of Fus in Kank2 RNA translation, we metabolically labeled cells with noncanonical amino acids (Dieterich et al., 2007). Cells were grown briefly (30 min) in the presence of azidohomoalanine (AHA; a methionine analogue) to label newly synthesized proteins. AHA-containing proteins were tagged with biotin by click-chemistry and purified. No biotinylated proteins were detected upon labeling with methionine or in the presence of the translation inhibitor cycloheximide (Fig. 2 d). Quantification of newly synthesized Kank2 or a control protein, from whole-cell extracts, normalized to their corresponding mRNA levels (detected through RT-PCR; Fig. 2 e), revealed that Fus silencing caused a significant decrease in the amount of protein produced from the Kank2 mRNA (Fig. 2 e). Therefore, Fus is required for efficient translation of the Kank2 mRNA.

Given that cytoplasmic Fus is present at cell protrusions (Fig. 1, d and e; and Fig. S1 c) and is able to regulate RNA translation (Fig. 2), we hypothesized that Fus might regulate translation preferentially within this cellular region. To test this idea, we devised the approach depicted schematically in Fig. 3 a. Cells were plated on microporous filters and sequentially labeled with homopropargylglycine (HPG) and AHA. Together with AHA, LPA was added to induce cell protrusion for 30 min. After fixation, Alexa Fluor 647 and Alexa Fluor 488 were coupled to HPG- and AHA-containing proteins, respectively, and protrusions and cell bodies were visualized. This approach allows

detection of two different protein pools, a preexisting, steady-state pool (red), and one newly synthesized as the cells extend protrusions (green). Both signals were specific, being significantly reduced in the presence of cycloheximide (Fig. 3 b). The preexisting protein pool served as an internal control for normalization of the newly synthesized protein signal. To determine preferential effects on translation within protrusions, we normalized the translation values within protrusions to those within the cell bodies (Fig. 3 d; see also Materials and methods). Interestingly, Fus KD cells showed a significant shift toward lower values of translation at protrusions. Importantly, this effect could be reversed by re-expression of shRNA-resistant wild-type Fus (Fig. 3, c and d).

Given that the above assay detects a ratio of new proteins, it was conceivable that lower ratios might result not from a decrease in translation at protrusions, but through an increase in translation of mRNAs in the cell bodies. In our hands the extent of AHA labeling showed significant variability among different experiments and thus was not optimal for directly comparing translation between different cell types. Therefore, we used puromycylation (Schmidt et al., 2009; David et al., 2012) to detect newly synthesized proteins and compared whole-cell translation between control and Fus KD cells (Fig. S2 a; whole-cell translation adequately reflects translation in cell bodies given that in our fractionations cell bodies contain ∼20-fold more cellular material compared with protrusions). Cells were exposed to puromycin for 5 min and nascent puromycylated proteins were detected with an anti-puromycin antibody. No puromycylated proteins were detected if puromycin was omitted or if the cells were pretreated with pactamycin (a translation initiation inhibitor) or anisomycin (a competitive inhibitor of puromycin). Significantly, no increase in the amount of puromycylated proteins (and thus translation efficiency) was observed in Fus KD cells. We do not rule out the possibility that some mRNAs in cell bodies also require Fus for efficient translation. However, taken together the above data strongly indicate that Fus is preferentially required for efficient translation within cell protrusions, consistent with its physical enrichment there (Fig. 1 e).

ALS-associated mutants of Fus preferentially recruit APC-RNPs in cytoplasmic granules

Dominant mutations in Fus cause ALS. These mutant proteins lead to formation of inclusions in neuronal cells, but their effect on cellular physiology is unknown (Lagier-Tourenne et al., 2010; Mackenzie et al., 2010). We sought to determine how ALS-associated mutations in Fus affect APC-RNPs. Upon transient expression, such mutants form cytoplasmic granules, which recapitulate to a certain extent the cytoplasmic inclusions found in patients. We expressed GFP- (or mRFP-) Fus carrying different ALS-associated mutations (R521C, R495X, or P525L) and immunostained for APC, as an APC-RNP marker. Remarkably, endogenous APC, detected using two different antibodies, as well as GFP-APC (not depicted), are efficiently recruited into mutant Fus granules (Fig. 4 a; and Fig. S2 b). FMRP, another APC-RNP component, was also present in mutant Fus granules, as was the stress granule marker TIA-1. The Wnt pathway components β-catenin and Axin and the P-body marker Dcp1a were absent (Fig. 4 a). These data suggest that the APC population recruited to cytoplasmic Fus granules is from APC-RNP complexes, and is distinct from the β-catenin destruction complex of the Wnt pathway.

Similarly, APC was recruited into mutant Fus granules in primary neuronal cells (Fig. 4 b). Additionally, we obtained tissue from patients with FTLD-Fus, a disease characterized by Fus cytoplasmic inclusions. These inclusions are absent from healthy donors and, significantly, are also immunoreactive for APC (Fig. 4 c). Thus, accumulation of APC in cytoplasmic granules is a bona fide characteristic of disease pathology.

To determine if RNAs present in APC-RNPs were also recruited into Fus granules we used an MS2-tagged reporter RNA that carries the Pkp4 3′UTR (β24bs/Pkp4), which is targeted to APC-RNPs (Mili et al., 2008). Indeed, the reporter RNA accumulates in mutant Fus granules. Interestingly, by FISH, the endogenous Ddr2 mRNA (an RNA associated with APC-RNPs [Mili et al., 2008]; Fig. S1, e and f) was robustly recruited into mutant Fus granules, whereas the control RhoA mRNA was recruited to a much lesser extent (Fig. 4 d), indicating that APC-RNPs are preferentially affected by ALS-associated Fus mutants.

APC-RNP transcripts are translated within cytoplasmic granules caused by either Fus overexpression or ALS mutants of Fus

Our initial expectation was that APC-RNPs recruited in mutant Fus granules would be translationally silenced, given that mutant Fus granules appear to correspond to stress granules, sites of translational repression (Andersson et al., 2008; Bosco et al., 2010; Dormann et al., 2010). Contrary to our expectation, however, expression of mutant Fus did not significantly affect the level of proteins encoded by several RNAs present in APC-RNPs (Kank2, Pkp4, and Ddr2; Fig. S3 a). Furthermore, immunostaining revealed that all these proteins were enriched within mutant Fus granules (Fig. 5 a). We thus entertained the opposite hypothesis, that RNAs recruited to mutant Fus granules are translationally active, leading to a local enrichment of the corresponding proteins. To test this, we briefly blocked translation with cycloheximide and assessed Kank2, Ddr2, and Pkp4 protein enrichment within mutant Fus granules (Fig. 5 a). Strikingly, this brief translation block caused a significant decrease in the amount of all three proteins within granules (Fig. 5 a).

As shown in Fig. 5 a, mutant Fus granules are not disrupted by cycloheximide treatment, and this is a characteristic of granules formed by several ALS-associated Fus mutants (Fig. S3 b). By contrast, cycloheximide rapidly leads to stress granule disassembly (Kedersha et al., 2000), further suggesting that Fus granules and stress granules possess different translational states.

To more directly test whether translation occurs within mutant Fus granules, we asked if newly synthesized, AHA-labeled proteins are concentrated there. Indeed, AHA labeling was concentrated within mutant Fus granules (Fig. 5 b). The observed signal was significantly reduced in the presence of cycloheximide, or if AHA was omitted, confirming its specificity

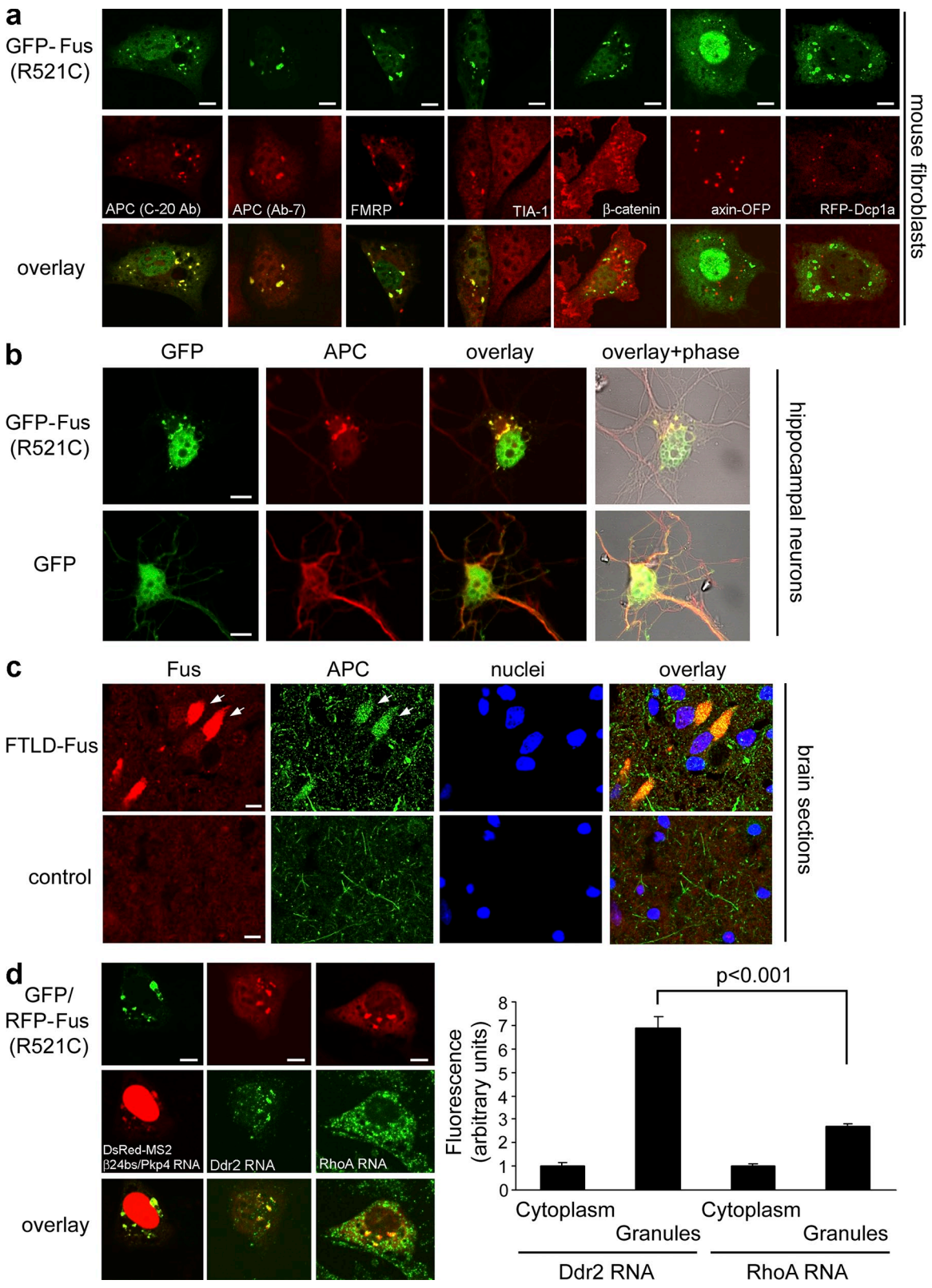

Figure 4. **Preferential recruitment of APC-RNPs in cytoplasmic granules formed by an ALS-associated mutant of Fus.** (a) NIH/3T3 cells were transfected with GFP-Fus(R521C) (top panels). Middle panels show distribution of coexpressed fluorescently tagged proteins or immunostaining of endogenous proteins. (b) Primary hippocampal neurons were transfected with GFP or GFP-Fus(R521C) and were immunostained at DIV5 to detect APC. (c) Hippocampal sections from a patient with FTLD-Fus (sporadic NIFID) and a control donor were stained for Fus and APC. Nuclei were stained with Draq5. Arrows point to Fus granules. Note that likely both glial cells and neurons are present in these sections. (d) NIH/3T3 cells transfected with GFP- or RFP-Fus(R521C) were analyzed by FISH to detect the Ddr2 or RhoA mRNAs or were cotransfected with DsRed-MS2 and an MS2 reporter RNA carrying the Pkp4 3′UTR (β24bs/Pkp4). Graph shows relative fluorescence intensities of Ddr2 and RhoA mRNAs within the cytoplasm or Fus granules. P-value is by Student's *t* test. Bars, 8 µm.

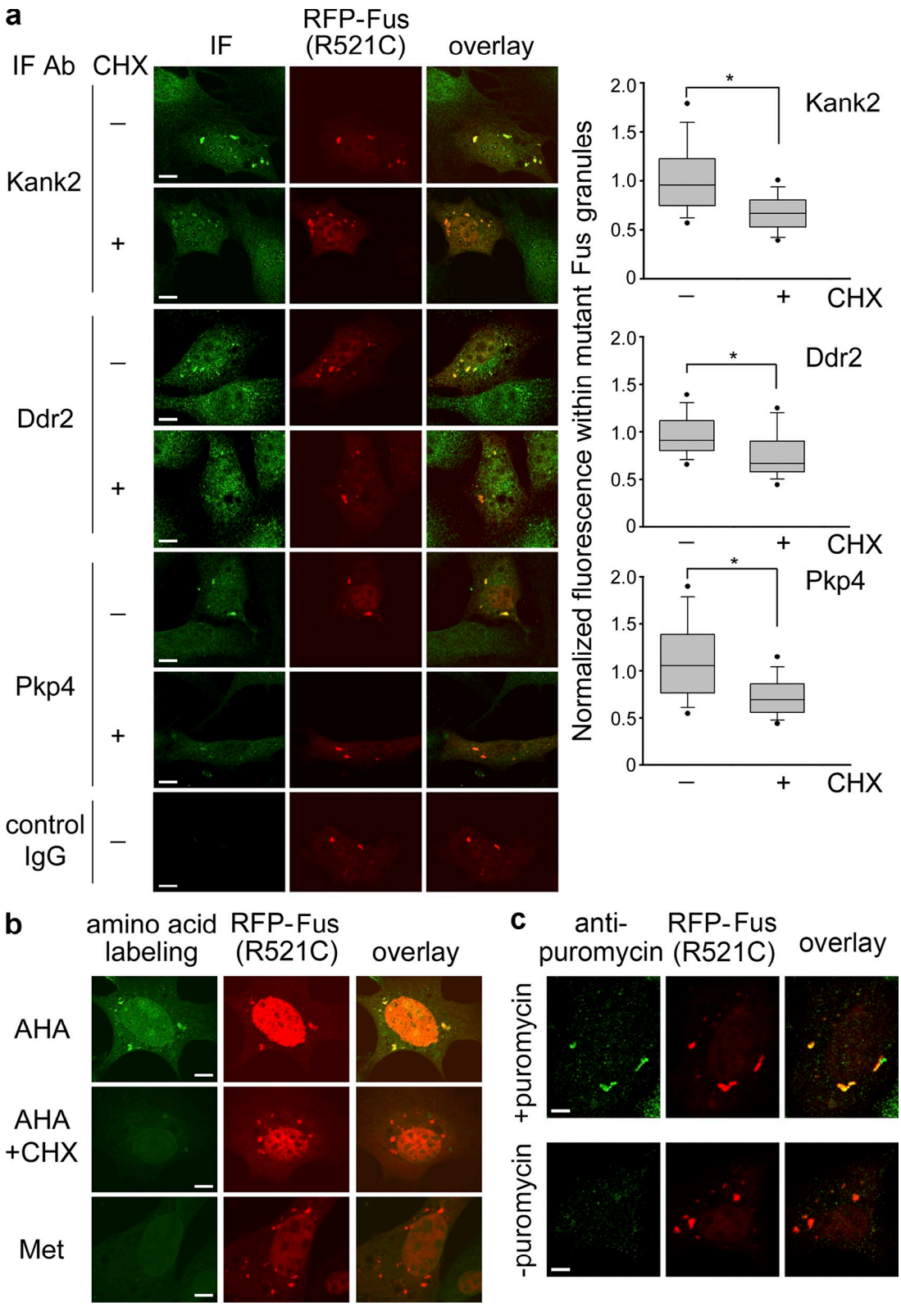

Figure 5. **Granules formed by mutant Fus are sites of active translation.** (a) Cells expressing RFP-Fus(R521C) were treated or not with cycloheximide (CHX) for 40 min and immunostained with the indicated antibodies (IF Ab). Box-plot graphs show fluorescence values within granules normalized to RFP-Fus signal. *, $P < 0.001$ by Mann-Whitney test. (b) Cells expressing RFP-Fus(R521C) were labeled for 30 min with AHA (with or without CHX) or with methionine (Met). After fixation, AHA-containing proteins were tagged with Alexa Fluor 488 and visualized. (c) Detection of translation sites in cells expressing RFP-Fus(R521C) using ribopuromycylation. Bars, 8 µm.

(Fig. 5 b). As an independent method, we used the ribopuromycylation (RPM) approach to visualize translating ribosomes (David et al., 2012). Consistent with our previous findings, mutant Fus granules coincided with sites of puromycin incorporation (i.e., translation sites) (Fig. 5 c). Pre-treatment of cells with pactamycin or anisomycin (which prevent puromycin incorporation into nascent proteins) significantly reduced the RPM signal (Fig. S3 c). No reduction was observed upon cycloheximide treatment, consistent with the ability of puromycin to be incorporated in stalled elongating ribosomes (Fig. S3 c; David et al., 2012). We conclude that, unexpectedly, Fus granules are sites of active RNA translation.

Apart from Fus mutations, overexpression of wild-type Fus has also been associated with disease in humans and in animal models (Huang et al., 2011; Mitchell et al., 2013; Sabatelli et al., 2013), suggesting that the increased presence and aggregation of the wild-type protein in the cytoplasm is sufficient to cause toxicity. Overexpression of wild-type Fus in fibroblast cells leads to formation of cytoplasmic granules, albeit in fewer cells compared with mutant Fus. Interestingly, wild-type Fus granules are similar to the mutant ones in terms of the recruitment of APC, FMRP, and Kank2 (Fig. S3 d) as well as the presence of translation sites (Fig. S3 e). Therefore, mislocalization of APC-RNPs appears to be a common consequence of Fus deregulation, caused by either mutation or overexpression.

Overall, we show here that under normal conditions cytoplasmic Fus is a component of APC-RNPs in cell protrusions and functions to promote their translation. Furthermore, cytoplasmic Fus granules, caused by ALS-linked mutations or by overexpression and which have similarities to stress granules, preferentially recruit APC-RNPs. This extends the notion that stress granules differ in their protein and RNA composition depending on the type of stress that induces their formation (Buchan et al., 2011; Damgaard and Lykke-Andersen, 2011). However, the striking distinction of cytoplasmic Fus granules concerns their translation status. Stress granules and higher order RNP particles have commonly been linked to translational repression (Anderson and Kedersha, 2008; Besse et al., 2009; Buchan and Parker, 2009). We show, quite unexpectedly, that RNAs within cytoplasmic Fus granules are translationally active, leading to local protein production from APC-RNPs. Our results indicate that active translation might be an unappreciated feature of RNA granules (Weil et al., 2012). Consistent with this idea, ribosomes have been observed in association with stress granules, and factors required for yeast stress granule assembly can positively influence mRNA translation (Gilks et al., 2004; Buchan et al., 2008). This study further suggests that misdirection of translation of specific RNA groups should be investigated as a potential toxic agent in Fus-mediated neurodegeneration.

Materials and methods

Plasmid constructs

To generate GFP-Fus, the coding sequence of mouse Fus was amplified by PCR and inserted into the SacI and BamHI sites of pEGFP-C1 (Takara Bio Inc.). To generate RFP-Fus, the NheI–SacI fragment, encoding GFP, was replaced with a NheI–SacI PCR-amplified fragment of mRFP. Point mutations were introduced using the QuikChange site-directed mutagenesis kit (Agilent Technologies). To generate Axin-OFP, PCR-amplified fragments of Axin and orange fluorescent proteins were introduced into the HindIII and NotI sites of pcDNA3. GFP-APC and RFP-Dcp1a have been described previously (Mili et al., 2008). GFP-APC contains human APC cDNA inserted into the SacI–BamHI sites of pEGFP-C1 (Takara Bio Inc.). For RFP-Dcp1a, a BamHI (blunted with T4 DNA polymerase)–NotI fragment of human DCP1a was ligated with a HindIII–NdeI (blunted with T4 DNA polymerase) fragment of mRFP into HindIII and NotI sites of pcDNA3 vector.

For knockdown experiments, control oligos targeting firefly luciferase or oligos targeting the mouse Fus mRNA were synthesized. The sequences are as follows: luciferase sense oligo: 5′-GATCCCC**CGTACGCGGAATACTTCGA**TTCAAGAGA**TCGAAGTATTCCGCGTACG**TTTTTGGAAA-3′; luciferase antisense oligo: 5′-AGCTTTTCCAAAAA**CGTACGCGGAATACTTCGA**TCTCTTGAA**TCGAAGTATTCCGCGTACG**GGG-3′; Fus sense oligo: 5′-GATCCCC**GCAACAAAGCTACGGACAA**TTCAAGAGA**TTGTCCGTAGCTTTGTTGC**TTTTTGGAAA-3′; Fus antisense oligo: 5′-AGCTTTTCCAAAAA**GCAACAAAGCTACGGACAA**TCTCTTGAA**TTGTCCGTAGCTTTGTTGC**GGG-3′. Bold characters indicate the targeting sequence; underlined characters indicate the 9-bp hairpin loop. The sense and antisense oligos were annealed and ligated into the BglII and HindIII sites of pSuper-retro-puro vector (Oligoengine). For re-expression of wild-type Fus into Fus KD cells, silent point mutations were introduced in the Fus cDNA, within the sequence targeted by the short hairpin RNA (GCAACA**GTCA**TA**T**GG**G**CA**G**; silent mutations in bold), using site-directed mutagenesis. The mutated Fus coding sequence was cloned into PmeI and SpeI sites of a modified gateway pENTR vector (Invitrogen) and was shuttled (using LR clonase; Life Technologies) into the lentiviral pINDUCER20 vector (Meerbrey et al., 2011). Expression of Fus in this vector is controlled under a doxycycline-inducible promoter.

Cell culture and transfection

NIH/3T3 cells were grown in DMEM supplemented with 10% calf serum, sodium pyruvate, penicillin, and streptomycin (Invitrogen). Plasmid constructs were transfected using Lipofectamine 2000 (Invitrogen) according to the manufacturer's instructions and cells were analyzed 24 h after transfection. For generation of knockdown cell lines, NIH/3T3 cells were transfected with pSuper-retro-puro plasmids, selected with 15 µg/ml puromycin (Sigma-Aldrich) for several days, and single cell clones were isolated and propagated.

For re-expression of Fus, Fus KD cells were transduced with pINDUCER20-Fus lentivirus and selected with 0.5 mg/ml Geneticin (Invitrogen). Before the experiment, expression of Fus was induced with addition of 500 ng/ml doxycycline.

For imaging of newly synthesized proteins within protrusions and cell bodies, or for isolation of these compartments, cells were plated on microporous filters and processed as described previously (Mili et al.,2008). Specifically, serum-starved cells were plated for 2 h on Transwell inserts (Costar) equipped with a 3-µm porous polycarbonate membrane, coated on both sides with 5 µg/ml fibronectin. For protein and RNA analysis, LPA was added in the bottom chamber for 1 h and the cells were fixed with 0.3% methanol-free formaldehyde (Polysciences, Inc.). Pseudopodia and cell bodies were scraped into cross-link reversal buffer (100 mM Tris, pH 6.8, 5 mM EDTA, 10 mM dithiothreitol, and 1% SDS), and the extracts were incubated at 70°C for 45 min and used for protein and RNA isolation. For labeling and visualization of newly synthesized proteins, cells on filters were processed as described below.

Hippocampi were dissected from embryonic day (E)19 rat embryos, trypsinized, and triturated through a glass Pasteur pipette. Dissociated neurons were plated on glass coverslips coated with 1 mg/ml poly-L-lysine. After initial attachment, the coverslips were transferred to dishes containing a monolayer of glia cells. Cultures were grown in neurobasal medium (Invitrogen) supplemented with B27 (Invitrogen) and 2 mM L-glutamine. Neurons were transfected at DIV4 using the calcium phosphate method.

Protein digestion and mass spectrometry

Visible bands were excised from the gel and cut into 1-mm × 1-mm pieces. These were washed 3× with water, 2× with 1:1 acetonitrile/100 mM ammonium bicarbonate, and dehydrated in 100% acetonitrile. After removing all acetonitrile, 30 µl of porcine trypsin (Promega) at a concentration of 20 µg/ml was added. After incubation on ice for 1 h the gel pieces were incubated at 37°C for 12–16 h. The supernatant was transferred to a second tube, and peptides were further extracted from the gel with acetonitrile. The two supernatants were mixed, then frozen and lyophilized. The peptides were redissolved in 5 µl of 1:1 acetonitrile/0.25% trifluoroacetic acid immediately before spotting on the MALDI target.

The matrix solution consisted of α-cyano-4-hydroxycinnamic acid (Sigma-Aldrich) saturating a solution of 1:1:0.02 acetonitrile/25 mM ammonium citrate in water/trifluoroacetic acid. Peptide (0.15 µl) was spotted on the MALDI target immediately followed by 0.15 µl matrix solution and allowed to dry. MALDI MS and MS/MS data were then acquired using a mass spectrometer (AB 4700 TOF/TOF; Applied Biosystems). Resultant peptide mass fingerprint and peptide sequence data were submitted to the NCBI database using the Mascot search engine.

Western blot and immunofluorescence

Antibodies used were as follows: anti-APC (C-20; Santa Cruz Biotechnology, Inc.), anti-APC (Ab-7; EMD Millipore), rabbit anti-Fus/TLS (Abcam), mouse anti-Fus/TLS (Proteintech), anti-FMRP (clone 1C3; EMD Millipore), rabbit-anti-β-catenin (Sigma-Aldrich), goat anti-Ddx5 (Abcam), rabbit anti-Kank2 (Proteintech), guinea pig anti-Pkp4 (also known as p0071; Progen), rabbit anti-Ddr2 (Abcam), rabbit anti-pY397-FAK (Biosource International), monoclonal anti-FAK (BD), and anti–α-tubulin (clone DM1A; Sigma-Aldrich). For immunofluorescence, NIH/3T3 cells were fixed for 15 min in 4% formaldehyde in PBS, permeabilized for 4 min in 0.2% Triton X-100 (or with 0.15 mg/ml digitonin as indicated), and blocked for 20–30 min in 3% BSA in PBS. Secondary antibodies were conjugated to Alexa Fluor 488 or Alexa Fluor 546 (Invitrogen).

Immunohistochemistry

Immunohistochemistry on human post-mortem material was performed on sections of formalin-fixed, paraffin-embedded tissue from hippocampus of FTLD-Fus patients or control individuals. Sections were de-paraffinized, rehydrated, boiled in Tris-EDTA buffer for antigen retrieval, blocked in 5% goat serum in PBS, and incubated with rabbit anti-Fus (Sigma-Aldrich) and anti-APC (CC-1; Abcam) antibodies. Draq5 (Cell Signaling Technology) was included in the last wash to stain the nuclei. Identical staining results were obtained when a wash of 1% Sudan Black B in 70% ethanol was included to quench tissue autofluorescence.

In situ hybridization

Cells were plated on fibronectin-coated glass slides for 2 h, fixed for 10 min with 4% formaldehyde in PBS, and dehydrated with ice-cold 70% ethanol at least overnight. Cells were rehydrated with 2× SSC in 50% formamide, prehybridized for 30 min at 50°C with hybridization buffer (50% formamide, 2× SSC, 10% dextran sulfate, 2 mM vanadyl ribonucleosides, 0.02% RNase-free BSA, 0.5 mg/ml *Escherichia coli* tRNA, and 0.2 mg/ml herring sperm DNA), and hybridized overnight at 50°C with 600 ng/ml digoxigenin-labeled riboprobes in hybridization buffer. Hybridized cells were washed at 50°C with 0.1× SSC in 50% formamide, incubated with HRP-conjugated anti-digoxigenin antibody (Roche), and the signal was amplified using the TSA-plus system (PerkinElmer). Slides were subsequently processed for immunofluorescence.

Antisense riboprobes were generated by in vitro transcription from PCR templates using the DIG RNA labeling kit (Roche). Riboprobes spanned the 3′UTR of the mouse RhoA mRNA, the whole coding sequence and 3′UTR of the mouse Rab13 mRNA, or the last coding exon and 1 kb of the 3′UTR of the mouse Ddr2 mRNA.

Immunoprecipitation and RT-PCR analysis

For immunoprecipitation, anti-APC (C-20; Santa Cruz Biotechnology, Inc.), anti-GFP (Molecular Probes), or control antibody (rabbit anti-HA tag; Santa Cruz Biotechnology, Inc.) were prebound on protein A beads together with 200 µg/ml *E. coli* tRNA, 200 µg/ml herring sperm DNA, 200 µg/ml RNase-free BSA, and 50 µg/ml glycogen for at least 1 h. Cells spreading on fibronectin-coated plates for ∼2 h were lysed in lysis buffer (10 mM Tris, pH 7.5, 100 mM NaCl, 2.5 mM $MgCl_2$, and 0.5% Triton X-100) supplemented with protease inhibitors (leupeptin, pepstatin, aprotinin) and RNase inhibitor (0.5 U/µl). Lysates were centrifuged at 10,000 *g* for 10 min and incubated with antibody-bound beads at 4°C for 3 h. Beads were washed 5× with lysis buffer and the immunoprecipitated material was released by incubation in lysis buffer containing 1% SDS. A fraction of the released material was analyzed by Western blot. Where indicated, the remainder was used for total RNA isolation (Trizol; Invitrogen) and RT-PCR analysis. RT-PCR conditions and primers have been described previously (Mili et al., 2008).

Labeling and analysis of newly synthesized proteins

For metabolic labeling and click chemistry, Click-iT reagents and buffers (Invitrogen) were used. For purification and Western blot analysis of newly synthesized proteins, cells were plated on fibronectin-coated plates and were grown for 40 min in methionine-free media. AHA was added to 200 µM for 30 min. Where indicated, cycloheximide was also included to 100 µg/ml, or AHA was substituted by methionine. Cells were lysed and sonicated in 100 mM Tris-Cl, pH 6.8, 5 mM EDTA, and 1% SDS. Part of the lysate was used for total RNA isolation (Trizol; Invitrogen) and RT-PCR analysis. The remainder was precipitated and processed for click-chemistry with biotin-alkyne (Invitrogen) according to the manufacturer's instructions. Biotinylated proteins were isolated on M280 streptavidin dynabeads (Invitrogen) and analyzed by Western blot. Band intensity was quantified using ImageJ software (National Institutes of Health). Normalized translation was calculated as the ratio of Kank2 protein/Kank2 RNA (each normalized to their corresponding loading controls).

For visualization of newly synthesized proteins, cells were grown in methionine-free media for 30 min and labeled with 200 µM AHA for 5–30 min, fixed, and processed for click-chemistry with Alexa Fluor 488 alkyne. Alternatively, serum-starved cells were plated on fibronectin-coated microporous filters and labeled with 300 µM HPG. HPG was washed off and 200 µM AHA was added. At the same time, 150 ng/ml LPA was added at the bottom chamber. Cells were allowed to extend protrusions for 30 min and were fixed and permeabilized. Click-chemistry reactions with Alexa Fluor 647 azide and Alexa Fluor 488 alkyne (Invitrogen) were sequentially performed according to the manufacturer's instructions. Cells on filters were subsequently processed for immunofluorescence and visualized by confocal microscopy. For image analysis, background values (from parallel experiments in the presence of cycloheximide) were subtracted and the ratio of AHA-Alexa488 to HPG-Alexa647 from multiple ROIs (>50 in each case) within protrusions or cell bodies was measured. To calculate the relative translation at protrusions the AHA/HPG ratio at protrusions was normalized to the median AHA/HPG value within cell bodies. Similar results were obtained in three independent experiments.

For Western blot analysis of puromycylated proteins, cells were incubated with 100 µg/ml puromycin for 5 min at 37°C. Where indicated, cells were pretreated for 15 min with 9.4 µM anisomycin or 0.5 µM pactamycin. Cells were immediately lysed on ice and analyzed by Western blot with the anti-puromycin 3RH11 monoclonal antibody (Kerafast).

For imaging translation sites with ribopuromycylation, cells were pretreated with 100 µg/ml cycloheximide for 15 min and 100 µg/ml puromycin was added for 5 min at 37°C. Cells were placed on ice, incubated for 2 min with permeabilization buffer (50 mM Tris-Cl, pH 7.5, 5 mM $MgCl_2$, 25 mM KCl, 100 µg/ml cycloheximide, 0.5 U/ml RNasin, and 0.015% digitonin), washed twice with permeabilization buffer, and fixed with 4% formaldehyde in PBS. Blocking and antibody-staining steps (3RH11 antibody; Kerafast) were performed in saponin-containing buffer (0.05% saponin, 10 mM glycine, and 5% FBS in PBS).

Image acquisition and analysis

Imaging was performed with a confocal microscope (LSM510 Meta; Carl Zeiss) operated by LSM-FCS software (Carl Zeiss) and equipped with a 40× Plan-Neofluar 1.3 NA oil objective. Samples were mounted with Fluoromount G medium (SouthernBiotech). EGFP or Alexa Fluor 488 were excited with the 488-nm line of an argon laser at 40% power, 5% transmission, and were detected using a bandpass 505–530-nm emission filter. RFP, OFP, and Alexa Fluor 546 were excited with the 543-nm line of a HeNe laser at 80% transmission and were detected using either a longpass 585-nm or a bandpass 560–615-nm emission filter. Alexa Fluor 647 was excited with the 633-nm line of a HeNe laser at 90% transmission and was detected using the Meta detector at a 649–724-nm window. Image analysis, ROI selection, and quantification were performed using ImageJ software.

Online supplemental material

Fig. S1 shows (a) Fus peptides identified through mass spectrum analysis (related to Fig. 1 a), (b) quantifications of Fus-RNA coimmunoprecipitations (related to Fig. 1 c), (c and d) additional examples of Fus-APC colocalization at protrusions (related to Fig. 1 e), and (e and f) effects of Fus knockdown on RNA localization at protrusions (related to Fig. 2). Fig. S2 shows (a) ribopuromycylation assay to assess total protein synthesis in control and Fus KD cells (related to Fig. 3) and (b) recruitment of APC in granules formed by the P525L and R495X Fus mutants (related to Fig. 4). Fig. S3 (related to Fig. 5) shows (a) effects on protein expression levels upon expression of mutant Fus, (b) lack of sensitivity of mutant Fus granules to cycloheximide treatment, (c) quantification of ribopuromycylation assay of Fig. 5 c, and (d and e) ribopuromycylation assay and proteins recruited in granules formed by overexpression of wild-type Fus. Online supplemental material is available at http://www.jcb.org/cgi/content/full/jcb.201306058/DC1. Additional data are available in the JCB DataViewer at http://dx.doi.org/10.1083/jcb.201306058.dv.

We thank Ian Mackenzie (University of British Columbia, Vancouver, BC, Canada) for generously providing tissue sections of ALS-Fus and FTLD-Fus patients and Mariann Bienz (MRC LMB, Cambridge, England, UK) for plasmids.

This work was supported by grant CA138905 from the NIH to S. Mili and grant HFSP-RGP0031 from the Human Frontier Science Program to I.G. Macara.

Submitted: 11 June 2013
Accepted: 29 October 2013

References

Anderson, P., and N. Kedersha. 2008. Stress granules: the Tao of RNA triage. *Trends Biochem. Sci.* 33:141–150. http://dx.doi.org/10.1016/j.tibs.2007.12.003

Andersson, M.K., A. Ståhlberg, Y. Arvidsson, A. Olofsson, H. Semb, G. Stenman, O. Nilsson, and P. Aman. 2008. The multifunctional FUS, EWS and TAF15 proto-oncoproteins show cell type-specific expression patterns and involvement in cell spreading and stress response. *BMC Cell Biol.* 9:37. http://dx.doi.org/10.1186/1471-2121-9-37

Bassell, G.J., and S.T. Warren. 2008. Fragile X syndrome: loss of local mRNA regulation alters synaptic development and function. *Neuron*. 60:201–214. http://dx.doi.org/10.1016/j.neuron.2008.10.004

Besse, F., S. López de Quinto, V. Marchand, A. Trucco, and A. Ephrussi. 2009. *Drosophila* PTB promotes formation of high-order RNP particles and represses oskar translation. *Genes Dev.* 23:195–207. http://dx.doi.org/10.1101/gad.505709

Blower, M.D., E. Feric, K. Weis, and R. Heald. 2007. Genome-wide analysis demonstrates conserved localization of messenger RNAs to mitotic microtubules. *J. Cell Biol.* 179:1365–1373. http://dx.doi.org/10.1083/jcb.200705163

Bosco, D.A., N. Lemay, H.K. Ko, H. Zhou, C. Burke, T.J. Kwiatkowski Jr., P. Sapp, D. McKenna-Yasek, R.H. Brown Jr., and L.J. Hayward. 2010. Mutant FUS proteins that cause amyotrophic lateral sclerosis incorporate into stress granules. *Hum. Mol. Genet.* 19:4160–4175. http://dx.doi.org/10.1093/hmg/ddq335

Buchan, J.R., and R. Parker. 2009. Eukaryotic stress granules: the ins and outs of translation. *Mol. Cell*. 36:932–941. http://dx.doi.org/10.1016/j.molcel.2009.11.020

Buchan, J.R., D. Muhlrad, and R. Parker. 2008. P bodies promote stress granule assembly in *Saccharomyces cerevisiae*. *J. Cell Biol.* 183:441–455. http://dx.doi.org/10.1083/jcb.200807043

Buchan, J.R., J.H. Yoon, and R. Parker. 2011. Stress-specific composition, assembly and kinetics of stress granules in *Saccharomyces cerevisiae*. *J. Cell Sci.* 124:228–239. http://dx.doi.org/10.1242/jcs.078444

Damgaard, C.K., and J. Lykke-Andersen. 2011. Translational coregulation of 5'TOP mRNAs by TIA-1 and TIAR. *Genes Dev.* 25:2057–2068. http://dx.doi.org/10.1101/gad.17355911

David, A., B.P. Dolan, H.D. Hickman, J.J. Knowlton, G. Clavarino, P. Pierre, J.R. Bennink, and J.W. Yewdell. 2012. Nuclear translation visualized by ribosome-bound nascent chain puromycylation. *J. Cell Biol.* 197:45–57. http://dx.doi.org/10.1083/jcb.201112145

Dieterich, D.C., J.J. Lee, A.J. Link, J. Graumann, D.A. Tirrell, and E.M. Schuman. 2007. Labeling, detection and identification of newly synthesized proteomes with bioorthogonal non-canonical amino-acid tagging. *Nat. Protoc.* 2:532–540. http://dx.doi.org/10.1038/nprot.2007.52

Dormann, D., R. Rodde, D. Edbauer, E. Bentmann, I. Fischer, A. Hruscha, M.E. Than, I.R. Mackenzie, A. Capell, B. Schmid, et al. 2010. ALS-associated fused in sarcoma (FUS) mutations disrupt Transportin-mediated nuclear import. *EMBO J.* 29:2841–2857. http://dx.doi.org/10.1038/emboj.2010.143

Gilks, N., N. Kedersha, M. Ayodele, L. Shen, G. Stoecklin, L.M. Dember, and P. Anderson. 2004. Stress granule assembly is mediated by prion-like aggregation of TIA-1. *Mol. Biol. Cell*. 15:5383–5398. http://dx.doi.org/10.1091/mbc.E04-08-0715

Harris, E.S., and W.J. Nelson. 2010. Adenomatous polyposis coli regulates endothelial cell migration independent of roles in beta-catenin signaling and cell-cell adhesion. *Mol. Biol. Cell*. 21:2611–2623. http://dx.doi.org/10.1091/mbc.E10-03-0235

Hengst, U., A. Deglincerti, H.J. Kim, N.L. Jeon, and S.R. Jaffrey. 2009. Axonal elongation triggered by stimulus-induced local translation of a polarity complex protein. *Nat. Cell Biol.* 11:1024–1030. http://dx.doi.org/10.1038/ncb1916

Holt, C.E., and S.L. Bullock. 2009. Subcellular mRNA localization in animal cells and why it matters. *Science*. 326:1212–1216. http://dx.doi.org/10.1126/science.1176488

Huang, C., H. Zhou, J. Tong, H. Chen, Y.J. Liu, D. Wang, X. Wei, and X.G. Xia. 2011. FUS transgenic rats develop the phenotypes of amyotrophic lateral sclerosis and frontotemporal lobar degeneration. *PLoS Genet.* 7:e1002011. http://dx.doi.org/10.1371/journal.pgen.1002011

Kedersha, N., M.R. Cho, W. Li, P.W. Yacono, S. Chen, N. Gilks, D.E. Golan, and P. Anderson. 2000. Dynamic shuttling of TIA-1 accompanies the recruitment of mRNA to mammalian stress granules. *J. Cell Biol.* 151:1257–1268. http://dx.doi.org/10.1083/jcb.151.6.1257

Kennell, J., and K.M. Cadigan. 2009. APC and beta-catenin degradation. *Adv. Exp. Med. Biol.* 656:1–12. http://dx.doi.org/10.1007/978-1-4419-1145-2_1

Kroboth, K., I.P. Newton, K. Kita, D. Dikovskaya, J. Zumbrunn, C.M. Waterman-Storer, and I.S. Näthke. 2007. Lack of adenomatous polyposis coli protein correlates with a decrease in cell migration and overall changes in microtubule stability. *Mol. Biol. Cell*. 18:910–918. http://dx.doi.org/10.1091/mbc.E06-03-0179

Lagier-Tourenne, C., M. Polymenidou, and D.W. Cleveland. 2010. TDP-43 and FUS/TLS: emerging roles in RNA processing and neurodegeneration. *Hum. Mol. Genet.* 19(R1):R46–R64. http://dx.doi.org/10.1093/hmg/ddq137

Lagier-Tourenne, C., M. Polymenidou, K.R. Hutt, A.Q. Vu, M. Baughn, S.C. Huelga, K.M. Clutario, S.C. Ling, T.Y. Liang, C. Mazur, et al. 2012. Divergent roles of ALS-linked proteins FUS/TLS and TDP-43 intersect in processing long pre-mRNAs. *Nat. Neurosci.* 15:1488–1497. http://dx.doi.org/10.1038/nn.3230

Leung, K.M., F.P. van Horck, A.C. Lin, R. Allison, N. Standart, and C.E. Holt. 2006. Asymmetrical beta-actin mRNA translation in growth cones mediates attractive turning to netrin-1. *Nat. Neurosci.* 9:1247–1256. http://dx.doi.org/10.1038/nn1775

Li, Z., L. Wang, T.S. Hays, and Y. Cai. 2008. Dynein-mediated apical localization of crumbs transcripts is required for Crumbs activity in epithelial polarity. *J. Cell Biol.* 180:31–38. http://dx.doi.org/10.1083/jcb.200707007

Liu-Yesucevitz, L., G.J. Bassell, A.D. Gitler, A.C. Hart, E. Klann, J.D. Richter, S.T. Warren, and B. Wolozin. 2011. Local RNA translation at the synapse and in disease. *J. Neurosci.* 31:16086–16093. http://dx.doi.org/10.1523/JNEUROSCI.4105-11.2011

Mackenzie, I.R., R. Rademakers, and M. Neumann. 2010. TDP-43 and FUS in amyotrophic lateral sclerosis and frontotemporal dementia. *Lancet Neurol.* 9:995–1007. http://dx.doi.org/10.1016/S1474-4422(10)70195-2

Meerbrey, K.L., G. Hu, J.D. Kessler, K. Roarty, M.Z. Li, J.E. Fang, J.I. Herschkowitz, A.E. Burrows, A. Ciccia, T. Sun, et al. 2011. The pINDUCER lentiviral toolkit for inducible RNA interference in vitro and in vivo. *Proc. Natl. Acad. Sci. USA*. 108:3665–3670. http://dx.doi.org/10.1073/pnas.1019736108

Mili, S., K. Moissoglu, and I.G. Macara. 2008. Genome-wide screen reveals APC-associated RNAs enriched in cell protrusions. *Nature*. 453:115–119. http://dx.doi.org/10.1038/nature06888

Mitchell, J.C., P. McGoldrick, C. Vance, T. Hortobagyi, J. Sreedharan, B. Rogelj, E.L. Tudor, B.N. Smith, C. Klasen, C.C. Miller, et al. 2013. Overexpression of human wild-type FUS causes progressive motor neuron degeneration in an age- and dose-dependent fashion. *Acta Neuropathol.* 125:273–288. http://dx.doi.org/10.1007/s00401-012-1043-z

Nagaoka, K., T. Udagawa, and J.D. Richter. 2012. CPEB-mediated ZO-1 mRNA localization is required for epithelial tight-junction assembly and cell polarity. *Nat Commun*. 3:675. http://dx.doi.org/10.1038/ncomms1678

Näthke, I.S. 2004. The adenomatous polyposis coli protein: the Achilles heel of the gut epithelium. *Annu. Rev. Cell Dev. Biol.* 20:337–366. http://dx.doi.org/10.1146/annurev.cellbio.20.012103.094541

Rogelj, B., L.E. Easton, G.K. Bogu, L.W. Stanton, G. Rot, T. Curk, B. Zupan, Y. Sugimoto, M. Modic, N. Haberman, et al. 2012. Widespread binding of FUS along nascent RNA regulates alternative splicing in the brain. *Sci Rep*. 2:603. http://dx.doi.org/10.1038/srep00603

Sabatelli, M., A. Moncada, A. Conte, S. Lattante, G. Marangi, M. Luigetti, M. Lucchini, M. Mirabella, A. Romano, A. Del Grande, et al. 2013. Mutations in the 3′ untranslated region of FUS causing FUS overexpression are associated with amyotrophic lateral sclerosis. *Hum. Mol. Genet.* 22:4748–4755. http://dx.doi.org/10.1093/hmg/ddt328

Sansom, O.J., K.R. Reed, A.J. Hayes, H. Ireland, H. Brinkmann, I.P. Newton, E. Batlle, P. Simon-Assmann, H. Clevers, I.S. Nathke, et al. 2004. Loss of Apc in vivo immediately perturbs Wnt signaling, differentiation, and migration. *Genes Dev.* 18:1385–1390. http://dx.doi.org/10.1101/gad.287404

Schmidt, E.K., G. Clavarino, M. Ceppi, and P. Pierre. 2009. SUnSET, a nonradioactive method to monitor protein synthesis. *Nat. Methods*. 6:275–277. http://dx.doi.org/10.1038/nmeth.1314

Shestakova, E.A., R.H. Singer, and J. Condeelis. 2001. The physiological significance of beta -actin mRNA localization in determining cell polarity and directional motility. *Proc. Natl. Acad. Sci. USA*. 98:7045–7050. http://dx.doi.org/10.1073/pnas.121146098

Vainer, G., E. Vainer-Mosse, A. Pikarsky, S.M. Shenoy, F. Oberman, A. Yeffet, R.H. Singer, E. Pikarsky, and J.K. Yisraeli. 2008. A role for VICKZ proteins in the progression of colorectal carcinomas: regulating lamellipodia formation. *J. Pathol.* 215:445–456. http://dx.doi.org/10.1002/path.2376

Weil, T.T., R.M. Parton, B. Herpers, J. Soetaert, T. Veenendaal, D. Xanthakis, I.M. Dobbie, J.M. Halstead, R. Hayashi, C. Rabouille, and I. Davis. 2012. *Drosophila* patterning is established by differential association of mRNAs with P bodies. *Nat. Cell Biol.* 14:1305–1313. http://dx.doi.org/10.1038/ncb2627